Tikrit Journal of Engineering Sciences (2023) 30 (3): 17-26

DOI: http://doi.org/10.25130/tjes.30.3.3

IRAQI Academic Scientific Journals

ISSN: 1813-162X (Print); 2312-7589 (Online)

Tikrit Journal of Engineering Sciences

available online at: http://www.tj-es.com

TJES Tikrit Journal of Engineering Sciences

Energy and Exergy Analyses of a Combined Power Plant Based on Natural Gas Combustion

Khalaf I. Hamada [a], Marwah N Mohammed [b], Raad R. Jasim [a], and Thamir K. Ibrahim [a]*

a Mechanical Engineering Department , Engineering College , Tikrit University ,Tikrit, Iraq

b Chemical Engineering Department , Engineering College , Tikrit University , Tikrit, Iraq

Keywords:

Combined Cycle, Combustion, Exergy Analysis, Greenhouse Gas, Natural Gas.

ARTICLE INFO

Article history:

Received:	04 May 2023
Received in revised form:	20 June 2023
Accepted:	29 June 2023
Final Proofreading:	05 Aug. 2023
Available online:	08 Aug. 2023

Citation: Hamada KI, Mohammed NM, Jasim RR, Ibrahim TK. Energy and Exergy Analyses of a Combined Power Plant Based on Natural Gas Combustion. *Tikrit Journal of Engineering Sciences* 2023; **30**(3): 17-26. http://doi.org/10.25130/tjes.30.3.3

Corresponding author:

Khalaf I. Hamada

Mechanical Department / Engineering College / Tikrit University /Tikrit, Iraq

Abstract: The present study implemented energy and exergy analyses on a 750MW combined cycle power plant (CCPP). The research utilized a simulation process using a computer model developed in MATLAB. The model was based on the natural gas combustion concept, energy balances, enthalpy balances, entropy changes, and the CCPPs heat transfer. The model was validated with the case study of the CCPP at Tuanku Ja'afar Power Station, Port Dickson. The results showed that the CCPP's energy and exergy efficiencies were 56% and 51%, respectively. Furthermore, applying exergy analysis revealed that the combustion chamber had a significant source of exergy destruction rate, i.e., 224.58 MW, which corresponded to 67.48% of the total exergy destruction in the CCPP, followed by the air compressor 7.53%, and the steam turbine 7.07%. Meanwhile, increasing the turbine inlet temperature (TIT) reduced the exergy destruction rate of the combustion chamber of the gas turbine cycle. The optimum performance obtained at TIT was higher than 1262 °C, where the exergy destruction decreased in the CCPP. Moreover, In CCPP, the combustion chamber was the highest exergy destruction rate, i.e., 225MW, among the main components of the power system. It can be grasped that the current adaptive model of natural gas combustion is a powerful tool for predicting the overall performance of the CCPPs based on exergy analysis.

تحليل الطاقة والاتاحية لمحطة توليد مشتركة على اساس احتراق الغاز الطبيعي

خلف ابراهيم حماده [1]، مروة نوري محمد [2] ، رائد رشاد جاسم [1]، ثامر خليل ابراهيم [1]
[1] قسم الهندسة الميكانيكية / كلية الهندسة / جامعة تكريت / تكريت, العراق.
[2] قسم الهندسة الكيمياوية/ كلية الهندسة / جامعة تكريت / تكريت, العراق.

الخلاصة

تضمنت الدراسة الحالية تحليلاً للطاقة والاتاحية لمحطة توليد ذات دورة مشتركة (CCPP) بسعة توليد 750 ميجاوات. استخدم البحث عملية محاكاة باستخدام نموذج حاسوبي تم تطويره ضمن بيئة الـ MATLAB. اعتمد النموذج على مفهوم احتراق الغاز الطبيعي، موازنة الطاقة، موازنة المحتوى الحراري، تغيرات الانتروبيا، التبادل الحرارية لمكونات الـ CCPPs. تم التحقق من صحة النموذج من خلال دراسة حالة لـ CCPP في محطة (Tuanku Ja'afar Power Station)، الواقعة في (Port Dickson). أظهرت النتائج أن كفاءات الطاقة والاتاحية لـ CCPP قيد الدراسة كانت 56٪ و 51٪ على التوالي. علاوة على ذلك، أظهر تطبيق تحليل الاتاحية أن غرفة الاحتراق لديها مصدر مهم لمعدل تدمير الطاقة، أي ما يعادل 224.58 ميجاوات ، والتي تمثل ما نسبته 67.48٪ من إجمالي تدمير الطاقة في الـ CCPP قيد الدراسة، يليها ضاغط الهواء بنسبة 7.53٪، والتوربينات البخارية بنسبة 7.07٪. بجانب ذلك، أدت زيادة درجة حرارة دخول الغازات المحترقة الى التوربين الغازي (TIT) إلى تقليل معدل تدمير الطاقة في غرفة الاحتراق لدورة التوربينات الغازية. كان الأداء الأمثل الذي تم الحصول عليه عندما كانت قيمة (TIT) أعلى من 1262 درجة مئوية، حيث انخفض تدمير الطاقة في الـ CCPP قيد الدراسة. علاوة على ذلك، كانت غرفة الاحتراق في الـ CCPP قيد الدراسة لها أعلى معدل تدمير للطاقة، أي 225 ميجاوات، من بين المكونات الرئيسية لنظام الطاقة. يمكن إدراك أن النموذج التكيفي الحالي لاحتراق الغاز الطبيعي هو أداة قوية للتنبؤ بالأداء العام لـ CCPPs بناءً على تحليل الاتاحية.

الكلمات الدالة: الدورة المشتركة، الاحتراق، تحليل الاتاحية، غازات الاحتباس الحراري، الغاز الطبيعي.

1.INTRODUCTION

A significant share of the world's energy demand is supplied by fossil fuel combustion. The widely used fossil fuels for power generation are coal, petroleum, and natural gas. Among these fuels, coal is the leading abundant resource for electricity generation worldwide. It was reported that about 42% of electricity generation worldwide is supplied mainly by coal combustion-based power plants. Furthermore, the coal consumption rate is expected to exceed six thousands of million tons of carbon equivalents by 2030 [1]. However, it is well-known that excessive carbon dioxide (CO_2) and other pollutants are emitted by coal combustion-based power plants' operation for electricity generation. The Canadian electricity generation reported that about one ton of CO_2 was emitted from coal burning to generate one MW of electricity. Such significant hazards of these aspects motivated governments and agencies to supply power plants based on more sustainable resources. Natural gas is one of these options due to its availability and suitability for existing technologies [2]. Practically, electricity generation based on fossil fuel combustion to operate a thermal plant has further challenges compared with a hydroelectric plant. The hydroelectric plant's working fluid should flow with extremely high pressure and temperature. Furthermore, continuous monitoring and repairing of its compound operating and control units are necessary to ensure the efficient working of the power plant with maximum power production [3].

The combined power plant can be defined as generating power in a higher thermodynamic cycle. However, some portion of its heat rejection is utilized to supply heat to a lower cycle. The upper cycle is frequently an open Brayton cycle for gas turbine, while the lower cycle is a steam turbine with a closed Rankine cycle. Joining both cycles produces a combined cycle power plant (CCPP) [4, 5]. In a combined cycle power plant, a gas turbine operates with primary fuel and works with a steam turbine to produce more electricity from the same amount of fuel. The gas turbine is connected to a heat recovery steam generator (HRSG), which uses exhaust heat that the gas turbine would otherwise release to the environment [6, 7]. HRSG is a series of heat exchangers comprising preheaters, economizers, evaporators, superheaters, and reheaters that absorb heat to create steam. Steam produced by HRSG is supplied to a different pressure level of steam turbines that drive the generator and produce electricity [8, 9]. The parameters of CCPP performance analysis, including exergy loss and energetic and exergetic efficiencies, evaluate and assess the CCPPs [10]. Determining the performance of a CCPP, excluding its components and overall system performance, is time-consuming and costly. The energy analysis carried out through a computed mathematical model is considered the most economical analysis method. In addition, it significantly contributes to the future design of the power generation industry. However, the CCPP is also analyzed by advanced thermodynamics topics, including exergy analysis [11,12]. Exergy analysis is a combination of the first and second laws of thermodynamics, highlighting the thermodynamics inefficiencies of a system.

Exergy analysis concentrates on the energy available in a system in a particular environmental condition. Its importance in the efficient use of energy resources has increased from year to year to identify the potential for improvement and energy saving. Exergy analysis is usually conducted by finding out the inefficient processes based on the exergy destruction rate of each component [13, 14]. The chemical and physical exergies at each point of the system are firstly determined by using the developed mathematical model and the thermodynamic properties of that point, such as temperature, pressure, flow rate, enthalpy, and entropy. Unlike the energy principle, exergy is not conserved within the system [15]. Exergy enables engineers in the power industry to acknowledge the interconnection between each system component. This detailed analysis is required to validate and improve the result's accuracy from the conventional exergy analysis [16, 17]. For instance, exergy analysis has become at the top of the thermodynamics cycle and a vital tool for the power cycle.

A complete assessment of a combined-cycle power plant working on natural gas was conducted by Cihan et al. [18], utilizing operational data from its units to undertake energy and exergy analysis. According to the data, the combustion chambers, gas turbines, and heat recovery steam generators (HRSG) were the principal sources of irreversibilities, accounting for more than 85% of total exergy losses. The influence of the pressure ratio and inlet gas turbine temperature on the exergy destruction and efficiency of a natural gas fired CCPP unit was performed by Reddy and Mohamed [19]. It was revealed that there was an optimum pressure ratio for a fixed inlet gas turbine temperature, which ensured minimum exergy destruction. Tang et al. [10] assessed the exergy destruction and efficiency of a natural gas-fired CCPP system coupled with post-combustion carbon capture (PCC) unit. It was revealed that more than 45% of the overall conventional CCPP system exergy destructed within the combustion chamber and condenser. On the other hand, comparatively great exergy destruction within the absorber of the PCC unit was recorded, i.e., 56%. Moreover, the highest exergetic efficiency recorded by the combustion chamber and heat recovery steam generator (HRSG) were 90% and 87%, respectively, while the lowest was recorded for the condenser. Ameri et al. [20] evaluated the components' irreversibilities of the Neka natural gas-fired CCPP (420 MW) based on the exergy concept. It was revealed that more than 83% of the Neka CCPP irreversibility's caused by the gas turbine, combustion chamber, HRSG, and duct burner. Among these components, the combustion chamber produced the highest exergy loss, followed by the HRSG. A definite potential enhancement of an electricity generation facility fuelled by natural gas was suggested by Açıkkalp et al. [21], based on the advanced approach of the exergy analysis. The system exergy efficiency and rate of destruction were estimated to be 40.2% and 78.242 MW, respectively. Four categories of exergy destruction, namely unavoidable, avoidable, exogenous, and endogenous, have been nominated to represent the total rate of the exergy destruction of the facility's components. A high ratio was recorded for the endogenous exergy rates, i.e., 70%, due to the weak interaction between the system's components. The overall potential for system improvement was 38%. The system's components with the highest enhancement potential were the combustion chambers, high-pressure steam turbine, and condenser.

Based on the survey of the previous studies, it was discovered that many studies were conducted to analyze various elements of the power plant, with the majority of them focusing on the analysis of HRSG and RBC. Several constructive and thermal recommendations for these devices have been suggested to improve system efficiency. However, it can be concluded that the energy analysis that solely depends on the first law of thermodynamics lacks the updated requirements that consider quality. Hence, the exergy analysis should be considered to involve quality and obtain accurate results of the CCPPs cycle. Therefore, in the present study, real-world data from Malaysia's Tuanku Jaafar Power Station (TJPS) were analyzed using energy and exergy analyses. Accordingly, this study investigates the elements of exergy destruction, determines the sources of loss, and provides remedies to improve the CCPP's efficiency and productivity.

2. PLANT DESCRIPTION

The modeled plant is the Tuanku Jaafar Power Station (TJPS), which consists of two blocks (A and B), each with a 750MW-combined cycle power plant. Each block was represented schematically, as shown in Fig. 1. The atmospheric air stream enters the compressor (C) at state 1, then is compressed into state 2, the combustion chamber (CC) entry. This air stream reacted with the injected fuel inside the combustion chamber and produced hot gases at state 3 with high heat energy. Part of this heat energy is converted into useful work at the gas turbine (GT), which is then converted into electrical power at the generator (G). A significant part of the remaining heat energy is exhausted with the hot gases from the GT at state 4, which enters the heat recovery steam generator (HRSG). Within the HRSG, there are three stages of heat recovery based on the high, intermediate, and low-pressure steam turbines.

Each recovery stage has a steam drum connected to an economizer, evaporator, reheater, and superheater. Furthermore, there are two steam deaerators for the high (SH-DeSH) and intermediate (RH-DeSH) stages besides the main cycle deaerator. The main cycle deaerator receives the condensed water from the condenser. Accordingly, the required steam amount could be generated to drive the high, intermediate, and low steam turbines. Also, there are two boiler feed pumps, i.e., the (HP/IP BFP) for the high and intermediate stages and the (IP BFP) for the low stages, to circulate the working fluid throughout the bottom steam cycle.

The diverter damper is vital in differentiating the plant using a closed (combined) or open (simple) cycle. The main purpose of the diverter damper is to provide safe and effective isolation of the HRSG from GT exhaust gas and to enable the GT simple cycle operation and combined cycle operation. A hydraulic diverter damper system is provided for each Gas Turbine, located between the Gas Turbine exhaust duct and the Heat Recovery Steam Generator inlet. Fig. 2 describes the operation diagram of the diverter damper. Two pairs of hydraulic cylinders are connected to lever arms to produce a pivot movement for the drive shaft.

3.ENERGY ANALYSIS

The above-mentioned CCPP's components were formulated based on the first law of thermodynamics and the mass conservation equations. Accordingly, the mass and energy balances for each component of the power plant operation system under the steady-state condition are expressed as [6, 7]:

$$\sum_{in} \dot{m} = \sum_{out} \dot{m} \quad (1)$$

$$\dot{Q} + \sum_{in} \dot{m}h = \dot{W} + \sum_{out} \dot{m}h \quad (2)$$

where $\dot{m}$, h, $\dot{W}$, and $\dot{Q}$ are mass flow rate, enthalpy, work output, and heat input, respectively. According to the symbols and notations described in Fig. 1, the final sets of governing equations for each component are summarized in Table 1. These equations were derived based on the steady-state operation condition for each component of the power plant system. The air and fuel mass flow rates were measured locally, while the exhaust gas flow rate was determined based on the conservation principle of mass, as follows:

$$\dot{m}_g = \dot{m}_a + \dot{m}_f \quad (3)$$

There are various values of the *LHV* (lower heating value) based on the used fuel specification. Natural gas, with specifications described in Table 2, was used as the fuel of the combustion chamber. The value of the *LHV* was considered equal (48806 kJ/kg) in the present study. The values of the specific heat of the air $(C_{p,a})$ and exhaust gas $(C_{p,g})$ were considered based on the following equations [6, 7]:

$$c_{p,a} = 1.0189 \times 10^3 - 0.13784T_a + (1.9843 \times 10^{-4})T_a^2 + (4.2399 \times 10^{-7})T_a^3 - (3.7632 \times 10^{-10})T_a^4 \quad (4)$$

$$c_{p,g} = 0.991615 + \left(\frac{6.99703T_g}{10^5}\right) + \left(\frac{2.7129T_g^2}{10^7}\right) - \left(\frac{1.22442T_g^3}{10^{10}}\right) \quad (5)$$

Table 1. Summary of the Governing Equations of the Energy Analysis [4, 5].

Plant Components		Energy Balanced Equation
Air compressor		$\dot{W}_{air-comp} = \dot{m}_a c_{p,a}(T_2 - T_1)$
Combustion chamber		$\dot{E}_f = \dot{m}_f . LHV_f$
Gas turbine		$\dot{W}_{GT} = \dot{m}_g c_{p,g}(T_3 - T_4)$
HRSG	HP	$\dot{m}_g c_{p,g}(T_{x_4} - T_{x_{10}}) = \dot{m}_{s,HP}(h_{A_{27}} - h_{A_{24}})$ $\dot{m}_g c_{p,g}(T_{x_3} - T_{x_4}) = \dot{m}_{s,HP}(h_{A_{28}} - h_{A_{27}})$ $\dot{m}_g c_{p,g}(T_4 - T_{x_3}) = \dot{m}_{s,HP}(h_{A_{31}} - h_{A_{28}})$
	IP	$\dot{m}_g c_{p,g}(T_{x_7} - T_{x_{10}}) = \dot{m}_{s,IP}(h_{A_{16}} - h_{A_{14}})$ $\dot{m}_g c_{p,g}(T_{x_6} - T_{x_7}) = \dot{m}_{s,IP}(h_{A_{17}} - h_{A_{16}})$ $\dot{m}_g c_{p,g}(T_{x_5} - T_{x_6}) = \dot{m}_{s,IP}(h_{A_{18}} - h_{A_{17}})$ $\dot{m}_g c_{p,g}(T_4 - T_{x_5}) = \dot{m}_{s,21}(h_{A_{23}} - h_{A_{20}})$
	LP	$\dot{m}_g c_{p,g}(T_{x_9} - T_{x_{10}}) = \dot{m}_{s,LP}(h_{A_{10}} - h_{A_9})$ $\dot{m}_g c_{p,g}(T_{x_8} - T_{x_9}) = \dot{m}_{s,LP}(h_{A_{11}} - h_{A_{10}})$ $\dot{m}_g c_{p,g}(T_{x_5} - T_{x_8}) = \dot{m}_{s,LP}(h_{A_{12}} - h_{A_{11}})$
Steam turbine		$\dot{W}_{ST} = \dot{m}_{w,HP}(h_{31} - h_{19}) + \dot{m}_{w,IP}(h_{23} - h_{32}) + [\dot{m}_{w,LP}h_{12} + \dot{m}_{w,IP}h_{32} - (\dot{m}_{w,IP} + \dot{m}_{w,LP})h_{33}]$
Condenser		$\dot{Q}_{cond} = (\dot{m}_{w,IP} + \dot{m}_{w,LP})(h_{33} - h_{34})$
Condensate pump		$\dot{W}_{cond.pump} = \dot{m}_6 h_6 - \dot{m}_{34}h_{34}$
LP BFP		$W_{LP,BFP} = \dot{m}_9 h_9 - \dot{m}_8 h_8$
HP/IP BFP		$\dot{W}_{HP/IP,BFP} = \dot{m}_{13}(h_{13'} - h_{13})$

Table 2. Composition of the Fuel Used (Natural Gas) [6, 7].

Fuel Components	Molar Percentages (%)
C	75.624
H	23.225
O	0
N	0.206
S	0
Moisture	0
Ash	0
CO_2	0.945

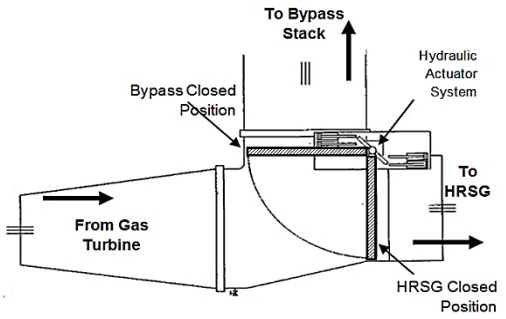

Fig. 2 Schematic of the Operation Diagram of the Diverter Damper.

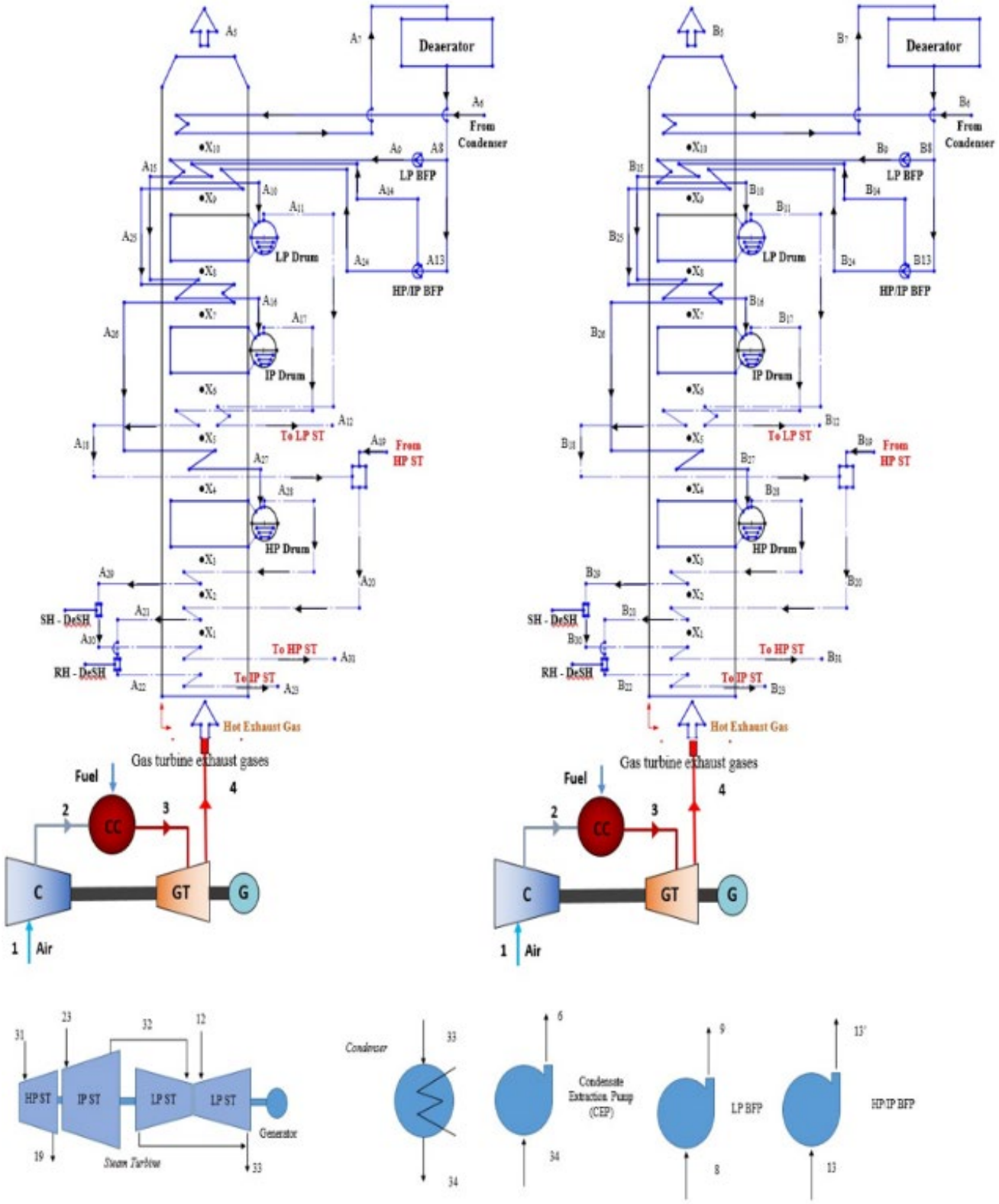

Fig. 1 Schematic Diagram of the Modeled CCPP.

4. Exergy Analysis

The main task of the present work is exergy analysis, which was performed based on the second law of thermodynamics. Essentially, four terms of exergy were considered, i.e., the kinetic, potential, physical, and chemical exergies. The maximum potential of a system to do the work at reference conditions represents the physical exergy. On the other hand, chemical exergy is related to the chemical composition change of a system from its equilibrium conditions. Chemical exergy is a vital part of combustion reactions. By applying the second laws of thermodynamics, the following equations are obtained [4, 5]:

$$\dot{E}_{x,heat} + \sum_i \dot{m}_i e_{x,i} = \sum_e \dot{m}_e e_{x,e} + \dot{E}_{x,w} + \dot{I}_{dest.} \quad (6)$$

$$\dot{E}_{x,heat} = \left(1 - \frac{T_0}{T_i}\right)\dot{Q}_i \quad (7)$$

$$\dot{E}_{x,W} = \dot{W} \quad (8)$$

$$e_x = e_{x,physical} + e_{x,chemical} \quad (9)$$

$\dot{E}_{x,heat}$ shows the exergy flow generated with heat transfer, $\dot{E}_{x,W}$ shows the exergy flow generated with work done by a system. The ambient environment condition is necessary for calculating the variation in a thermodynamic property (First Law analysis). However, exergy analysis cannot be conducted without identifying the ambient condition, which varies from place to place. In this study, the temperature and pressure of the environment are considered as 298 K and 101.3 kPa. The ambient reference model for air used in the present analysis is given in Table 3 [22]. For the water/steam phases, the equation below is used to evaluate the physical exergy [6, 7]:

$$e_{x,physical} = (h - h_0) - T_0 (s - s_0) \quad (10)$$

(h_0) and (s_0) represent the values of the systems' enthalpy and entropy, respectively, under the environment condition (at dead-state conditions). On the other hand, the physical exergy of the gas was calculated using the physical exergy equations of ideal gases, as follows [2]:

$$e_{x,physical} = e_x^T + e_x^P \quad (11)$$

$$e_x^T = c_p\left[(T - T_0) - T_0 \ln\frac{T}{T_0}\right] \quad (12)$$

$$e_x^P = RT_0 \ln\frac{P}{P_0} \quad (13)$$

Accordingly, the terms of the physical exergy rates, i.e., (e_x^T) and (e_x^P), were evaluated based on an ideal gas mixture's temperature and pressure, respectively.

Table 3. Molar Percentages and Standard Chemical Exergy of the Constituents in Atmospheric Air [22].

Constituents	Molar percentages (%)	Chemical Exergy (kJ/mol)
CO_2	0. 03	19.87
H_2O	1.90	9.49
O_2	20. 59	3.97
N_2	77.48	0.72

The combustion products are assumed as an ideal gas mixture through analysis. To calculate the chemical exergy of a mixture, it is crucial to know the molar composition of the combustion gases after the combustion process. Therefore, the combustion gases' molar composition was determined based on the actual combustion equation by considering the measured flow rates of air and fuel. Moreover, the actual composition of the natural gas (see Table 2) and the ambient reference model for air (see Table3) were adopted for analysis. Accordingly, the corresponding reaction equation of the actual combustion process of the natural gas within the combustion chamber proposed by Bejan et al. [23] is:

$$\begin{aligned}\bar{\lambda}(y_{f,C}C + y_{f,H}H + y_{f,N}N + y_{f,CO_2}CO_2) \\ + (y_{a,N_2}N_2 + y_{a,O_2}O_2 + y_{a,H_2O}H_2O \\ + y_{a,CO_2}CO_2) \\ \rightarrow (1+\bar{\lambda})(y_{p,N_2}N_2 + y_{p,O_2}O_2 \\ + y_{p,H_2O}H_2O + y_{p,CO_2}CO_2)\end{aligned} \quad (14)$$

where y_a, y_f, and y_p represent the molar fraction of the components of the air, fuel, and combustion products, respectively. Also $\bar{\lambda}$, represents the molar fuel-air ratio of the feeding mixture of the CCPP, which is evaluated by Bejan et al. [23]:

$$\frac{\dot{m}_f}{\dot{m}_a} = \frac{(\sum \dot{n}_i . M_i)_f}{(\sum \dot{n}_i . M_i)_a} = \bar{\lambda}\frac{M_f}{M_a} \quad (15)$$

$$\therefore \bar{\lambda} = \frac{\dot{n}_f}{\dot{n}_a} = \frac{\dot{m}_f}{\dot{m}_a} \times \frac{M_a}{M_f} \quad (16)$$

The corresponding mole fractions of the combustion products are defined based on the atomic balance of the reacted elements, which are summarized below:

$$y_{p,CO_2} = \frac{0.0003 + 0.76569\bar{\lambda}}{1+\bar{\lambda}} \quad (17)$$

$$y_{p,H_2O} = \frac{0.019 + 0.116125\bar{\lambda}}{1+\bar{\lambda}} \quad (18)$$

$$y_{p,O_2} = \frac{0.2059 - 0.8143025\bar{\lambda}}{1+\bar{\lambda}} \quad (19)$$

$$y_{p,N_2} = \frac{0.7748 + 0.00103\bar{\lambda}}{1+\bar{\lambda}} \quad (20)$$

Finally, the net chemical exergy of a gas mixture is evaluated as follows [24]:

$$ex^{ch} = \sum_{i=1}^{n} y_i ex_i^{ch} + RT_0 \sum_{i=1}^{n} y_i \ln y_i \quad (21)$$

The specific chemical exergy of the fuel (natural gas) proposed by [10] is:

$$\zeta = \frac{ex_{\text{fuel}}^{ch}}{LHV_{\text{fuel}}} \quad (22)$$

where the term (ζ) is the ratio of the fuel's chemical exergy to its LHV. Generally, the value of (ζ) is considered 1.06 for natural gas [4, 5]. According to the symbols and notations described in Fig. 1, a summary of the exergy analysis for each component is briefed in Table 4 in terms of the exergy destruction rate and Table 5 in terms of exergy efficiency.

Table 4. Summary of Exergy Destruction Rate Equations [4, 5].

Plant Components	Exergy Destruction Rate
Air compressor	$\dot{I}_{dest,comp} = \dot{W}_{comp} - (\dot{E}_{x,2} - \dot{E}_{x,1})$
Combustion chamber	$\dot{I}_{dest,CC} = \dot{E}_{x,f} - (\dot{E}_{x,3} - \dot{E}_{x,2})$
Gas turbine	$\dot{I}_{dest,GT} = (\dot{E}_{x,3} - \dot{E}_{x,4}) - \dot{W}_{GT}$
HRSG	$\dot{I}_{dest,HRSG} = (\dot{E}_{x,4} - \dot{E}_{x,5}) - (\dot{E}_{x,12} - \dot{E}_{x,9}) - (\dot{E}_{x,18} - \dot{E}_{x,14}) - (\dot{E}_{x,23} - \dot{E}_{x,19} - \dot{E}_{x,18}) - (\dot{E}_{x,31} - \dot{E}_{x,24})$
Steam turbine	$\dot{I}_{dest,ST} = (\dot{E}_{x,31} - \dot{E}_{x,19}) + (\dot{E}_{x,23} - \dot{E}_{x,32}) + (\dot{E}_{x,12} + \dot{E}_{x,32} - \dot{E}_{x,33}) - \dot{W}_{ST}$
Condenser	$\dot{I}_{dest,cond} = (\dot{E}_{x,33} - \dot{E}_{x,34}) + (\dot{E}_{x,cw,i} - \dot{E}_{x,cw,o}) - \dot{Q}_{cond}\left(1 - \frac{T_0}{T}\right)$
Condensate pump	$\dot{I}_{dest,cond.pump} = \dot{W}_{cond.pump} - (\dot{E}_{x,6} - \dot{E}_{x,34})$
LP BFP	$\dot{I}_{dest,LP,BFP} = \dot{W}_{LP,BFP} - (\dot{E}_{x,9} - \dot{E}_{x,8})$
HP/IP BFP	$\dot{I}_{dest,HP/IP,BFP} = \dot{W}_{HP/IP,BFP} - (\dot{E}_{x,13'} - \dot{E}_{x,13})$

Table 5. Summary of Exergy Efficiency of Plant Components [4, 5].

Plant Components	Exergy Efficiency
Air compressor	$\eta_{ex,AC} = \frac{\dot{E}_{x,2} - \dot{E}_{x,1}}{\dot{W}_{comp}}$
Combustion chamber	$\eta_{ex,CC} = \frac{\dot{E}_{x,3} - \dot{E}_{x,2}}{\dot{E}_{x,f}}$
Gas turbine	$\eta_{ex,GT} = \frac{\dot{W}_{GT}}{\dot{E}_{x,3} - \dot{E}_{x,4}}$
HRSG	$\eta_{ex,HRSG} = \frac{\left[(\dot{E}_{x,A_{12}} - \dot{E}_{x,A_9}) + (\dot{E}_{x,A_{18}} - \dot{E}_{x,A_{14}}) + (\dot{E}_{x,A_{23}} - \dot{E}_{x,A_{19}} - \dot{E}_{x,A_{18}}) + (\dot{E}_{x,A_{31}} - \dot{E}_{x,A_{24}})\right]}{\dot{E}_{x,4} - \dot{E}_{x,5}}$
Steam turbine	$\eta_{ex,ST} = \frac{\dot{W}_{ST}}{\left[(\dot{E}_{x,31} - \dot{E}_{x,19}) + (\dot{E}_{x,23} - \dot{E}_{x,32}) + (\dot{E}_{x,12} + \dot{E}_{x,32} - \dot{E}_{x,33})\right]}$
Condenser	$\eta_{ex,cond} = 1 - \frac{\dot{I}_{dest,Cond}}{\left[(Ex_{33} - Ex_{34}) + (Ex_{cw,i} - Ex_{cw,o})\right]}$
Condensate pump	$\eta_{ex,cond.pump} = \frac{\dot{E}_{x,6} - \dot{E}_{x,34}}{\dot{W}_{cond.pump}}$
LP BFP	$\eta_{ex,LP,BFP} = \frac{\dot{E}_{x,9} - \dot{E}_{x,8}}{\dot{W}_{LP,BFP}}$
HP/IP BFP	$\eta_{ex,HP/IP,BFP} = \frac{\dot{E}_{x,13'} - \dot{E}_{x,13}}{\dot{W}_{HP/IP,BFP}}$

5. Results and Discussions

In the preceding section, the CCPP's mathematical models were developed based on the energy and exergy concepts. These models were executed based on an actual data set from the CCPP at the Tuanku Jaa'far Power Station as a case study. A sample of this data set is presented in Table 6. The selected points represent the inlet and outlet conditions of the working fluids in the main components of the upper gas and bottom steam cycles. The thermodynamic properties and thermal efficiency of the power cycle were calculated based on energy analysis using energy and mass-balanced equations. Exergy that is destroyed within each component's system and exergy efficiency were determined to study the irreversibilities of the system and identify the chances to enhance the power system.

Table 6. Thermodynamics Properties of Selective Point in the CCPP.

Point	P (kPa)	T (°C)	ṁ (kg/s)	h_{H2O} (kJ/kg)
1	101.3	30	604.62	-
2	1335.9	440	604.62	-
3	1335.9	1250	617.83	-
4	101.3	606	617.83	-
5	101.3	106	617.83	-
12	550	255	22.44	2969.8
19	3870	367.80	152.06	3141.5
23	3500	566	168.56	3599.6
31	12500	538	152.06	3443.4
32	500	260	168.56	2981.8
33	8	41.90	191	2400.7

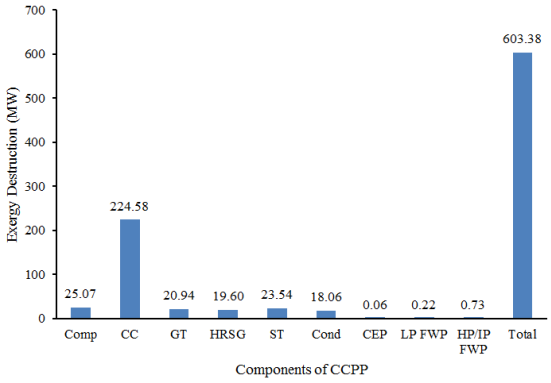

Fig. 3 Exergy Destruction Occurs in Each Component of CCPP.

Table 7 shows the energy analysis result on the CCPP using the mass and energy balance equations formed in the previous section. It can be observed that the work required for the compressor was 250MW to compress the air inlet into a desired operational condition for the upper gas cycle. A chemical reaction occurred within the combustion chamber between the fuel (natural gas), with a net entering energy of nearly 650MW, and the compressed air to produce 900MW of energy at the exit.

Table 7. Result of the Energy Analysis of the Modeled CCPP.

Component	W_{in} (kW)	W_{out} (kW)	Q_{in} (kW)	Q_{fuel} (kW)	Q_{out} (kW)
Compressor	250063.21	-	18211.54	-	267096.31
Combustion Chamber	-	-	267096.31	644644.29	911255.01
Gas Turbine	-	477974.40	911255.01	-	441637.63
HRSG	-	-	441637.63	-	77274.42
Steam Turbine	-	260759.96		-	458533.70
Condenser	-	-	458533.70	-	33554.87
Condensate Pump	332.34	-	33150.67	-	33483.01
LP BFP	321.97	-	11761.83	-	12083.79
HP/IP BFP	1991.66	-	95092.39	-	97084.05

The combustion gases produced drove the turbine blades in the gas turbine (GT), generating about 480MW of power output for

each cycle. Hence, the network produced by the gas cycle was in the range of 220 and 230MW after considering the compressor work's usage. In the open cycle of the Tuanku Jaa'far Power Station, when the diverter damper is opened, the gas turbine exhaust is released into the environment. In this case, the thermal efficiency is calculated only for the network generated by the gas turbine, which was around 34 - 35%, and about 450MW of heat energy was lost to the surrounding. However, when the damper is closed, the exhaust gas enters the heat recovery steam generator, which acts as the heat exchanger that transfers the waste heat energy to the second working fluid to produce superheated steam and run the steam turbine [6, 7]. The additional work generated by the steam turbine was about 260MW and 3MW of the work required to run the pumps in the steam cycle, such as low-pressure, intermediate, and high-pressure boiler feed water pumps and condensate extraction pump [4]. Consequently, the thermal efficiency of the power plant could rise to 55%, and the waste heat energy loss to the environment was remarkably reduced to 80MW.

The exergy analysis results in Fig. 3 demonstrate that the combustion chamber significantly dominated the exergy destruction in the CCPP modeled due to the chemical reaction between the burning fuel and the compressed air, which is attributed to the significantly associated irreversibilities [6, 7]. Hence, the most inefficient component was the combustion chamber. Since the combustion process is the major source of the high exergy destruction rate within the CC, it is vital to reveal the variation of the chemical and physical exergy at the exit of the CC (state 3 in Fig. 1) with a certain parameter [18, 19]. This indicates the existence of high potential improvement in the component toward the better performance of the power system [10, 20]. In the meantime, the other components should be considered despite their insignificant contribution to the total exergy destruction rate of the entire system because any reduction in the destruction rate of the system's exergy improves the overall efficiency of the CCPP [4, 5].

As discussed above, the destruction rate of the exergy within the CC is contributed by the enormous exergy value at state 3 that resulted from the combustion gas production at a high temperature reaching 1300°C. The variation of the physical exergy and exergy destruction rate at point 3 versus the inlet temperature of the gas turbine was investigated, as shown in Fig. 4. At a constant pressure ratio, the exergy amount at the combustion chamber exit increased with the inlet temperature of the gas turbine. Thus, based on the governing equation (row #2 in Table 4), the exergy destruction rate within the combustion chamber decreased, as illustrated in Fig. 4. The cross point between the curves of the exergy and the rate of exergy destruction at point 3 versus the gas turbine inlet temperature was at 1262°C. It can be seen that the best performance was achieved when the temperature was higher than 1262°C, where the exergy destructed in the combustion chamber was reduced.

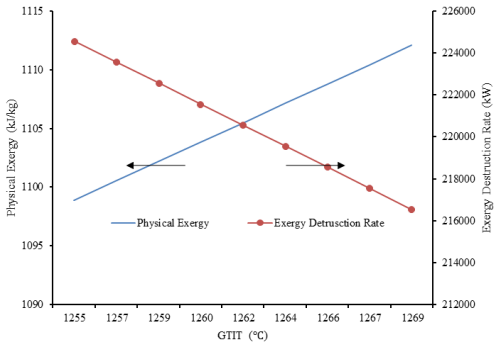

Fig. 4 Physical Exergy and Exergy Destruction Rate versus Inlet Temperature of the Gas Turbine.

The irreversibility percentages of the combustion chamber, compressor, steam turbine, gas turbine, HRSG, condenser, and pumps are shown in Fig. 5. The components' irreversibilities were evaluated based on actual data from the CCPP operation. By conducting the experiments in time series, it was found that the combustion chamber was the primary exergy destruction component in the system, with about 67%, followed by the compressor and turbines. The pie chart in Fig. 5 clearly shows the percentage distribution of the destruction rate exergy among the components in the combined power cycle. As expected, the contribution of condensate extraction pumps and triple pressure level boiler feed water pumps towards the total exergy loss in the power cycle was less than 0.5%, which was negligible and worth no effort to improve. On the other hand, the HRSG and condenser are the components of the upper steam cycle with a high chance of being enhanced as the exergy was destroyed in the system, essentially caused by the temperature difference in the heat exchanger [10, 20]. Furthermore, the heat energy loss to the environment can be utilized

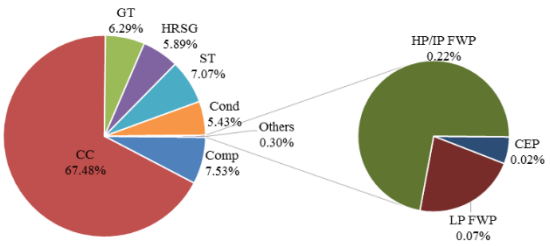

Fig. 5 Percentage of Exergy Destruction Rate for Each Component in the CCPP.

for district heating and cooling system and increase the overall efficiency [25, 26].

In Fig. 6, the combination of each component exergy's destruction rate and efficiency in the modeled CCPP is graphically presented. It can be observed that the higher the exergy destroyed within a system, the lower the exergy efficiency of the components. It is revealed that the FWP condenser and combustion chamber had the lowest exergetic efficiency, i.e., below 70%. Among these components, the LPFWP had the lowest efficiency, i.e., about 31%, while the combustion chamber had the highest, i.e., about 67%. However, regarding the exergy destruction, the combustion chamber caused approximately the major rate of 225MW. This large loss of useful work in the combustion chamber is mainly because of the high-temperature level of the system related to the equilibrium state [18-20]. The occurrence of the fuel-air mixture's chemical reaction also contributed to a certain amount of loss. Therefore, it could be concluded that the overall exergetic efficiency of the CCPP system was largely influenced by the combustion chamber [4, 5]. Recently, the importance of the exergy aspect cannot be negligent not only because of the accuracy that can be achieved by it, but also because of its economic and environmental consequent results. The exergy and its consequent calculations provide a comprehensive figure for the decision-makers and investors to take their verdict, making our world healthier and safer [27]. For the overall CCPP, the exergy efficiency was about 51%, less than the corresponding energy efficiency of

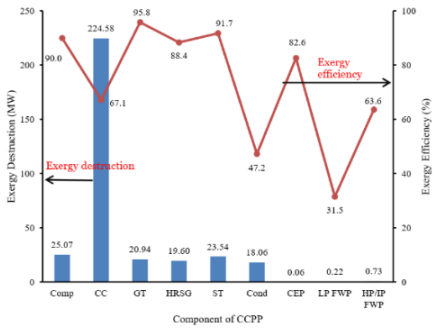

Fig. 6 Destruction Rate and Efficiency of the Components' Exergy in the CCPP.

55%.

6.CONCLUSIONS

1. 450MW and 80MW of heat energy were released to the surroundings for the open and closed cycles, respectively. This release occurred because of the advantage of a heat recovery steam generator that converted most of the waste energy to the second working fluid, which operated the steam turbines with superheated steam at various pressure levels.
2. The Energetic thermal efficiency of the CCPP was enhanced by around 60% due to the steam cycle effect. In addition, applying the steam cycle reduced the loss of the CCPP plant by about 81%.
3. The combustion chamber had the major exergy destruction that, was about 225MW of fuel exergy (67.5% of the total exergy destruction in the power cycle), followed by the compressor, about 7.53% and 7.07% from the steam turbine, and less than 7% for each of the other components.
4. The exergy destruction rate of the combustion chamber was reduced when the gas turbine inlet temperature increased due to a higher exergy value at the exit of the combustion chamber at a high temperature of the gas turbine inlet.

ACKNOWLEDGMENTS

The authors would like to thank the Tuanku Ja'afar Power Station staff at Port Dickson for providing the raw operational data to achieve the present study. Furthermore, the authors would like to thank Tikrit University for its fund support.

REFERENCES

[1] IEA, ***Electricity Market Report-January*** 2022, in, IEA Paris, France, 2022.

[2] Dincer, I., Rosen, M.A **Chapter 13 - *Exergy analyses of cogeneration and district energy systems, in: Dincer*, I. & Rosen, M.A. (eds.) Exergy (Third Edition)**, Elsevier, 2021, pp. 285-302. doi: 10.1016/j.applthermaleng.2004.05.008

[3] Salih WA, Alkumait AA, Khalaf HJ. **Energy and Exergy Assessment of North Refineries Company (NRC) Steam Cycle Based on Air Mass Flowrate of Main Condenser**. *Tikrit Journal of Engineering Sciences* 2021; **28** (3): 61-70. doi: 10.25130/tjes.28.3.05.

[4] Shireef LT, Ibrahim TK. **Influence of Operating Parameters on the Performance of Combined Cycle Based on Exergy Analysis**. *Case Studies in Thermal Engineering* 2022; **40**, 102506. doi: 10.1016/j.csite.2022.102506

[5] Ibrahim TK, Mohammed MK, Awad OI, et al. **A Comprehensive Review on the**

Exergy Analysis of Combined Cycle Power Plants. *Renewable and Sustainable Energy Reviews* 2018; **90**: 835-850. doi: 10.1016/j.rser.2018.03.072

[6] Altarawneh, O. R., Alsarayreh, A. A., Ala'a, M., Al-Kheetan, M. J., & Alrwashdeh, S. S. **Energy and Exergy Analyses for a Combined Cycle Power Plant in Jordan**, *Case Studies in Thermal Engineering* 2022; **31**: 101852. doi: 10.1016/j.csite.2022.101852

[7] Bataineh K, Khaleel BA. **Thermodynamic Analysis of a Combined Cycle Power Plant Located in Jordan: A Case Study**, *Archives of Thermodynamics* 2020; **41**(1): 95-123. doi: 10.24425/ather.2020.132951

[8] Param HK, Jianu OA. **Exergy Analysis of Heat Recovery Steam Generator: Effects of Supplementary Firing and Desuperheater**, *ASME Journal of Energy Resources Technology* 2020; **142**(5): 050908 (10 pages). doi:10.1115/1.4046084

[9] Maruf MH, Rabbani M, Ashique RH, et al. **Exergy Based Evaluation of Power Plants for Sustainability and Economic Performance Identification**. *Case Studies in Thermal Engineering* 2021; **28**(December): 101393.

[10] Tang, Y., Chong, C. T., Li, J., Ng, J. H., & Herraiz, L. **Analysis of a Natural Gas-Fired Gas Turbine Combined Cycle Power Plant with Post-Combustion Carbon Capture.** *Chemical Engineering Transactions* 2021; **83**: 529-534. doi: 10.3303/CET2183089

[11] Khaleel, O. J., Ismail, F. B., Ibrahim, T. K., & bin Abu Hassan, S. H. **Energy and Exergy Analysis of the Steam Power Plants: A Comprehensive Review on the Classification, Development, Improvements, and Configurations**. *Ain Shams Engineering Journal* 2022; **13(3)**: 101640. doi: 10.1016/j.asej.2021.11.009

[12] Khaleel OJ, Ismail FB, Ibrahim TK, Al-Sammarraie AT. **Developing an Analytical Model to Predict the Energy and Exergy Based Performances of a Coal-Fired Thermal Power Plant.** *Case Studies in Thermal Engineering* 2021; **28**: 101519. doi: 10.1016/j.csite.2021.101519

[13] Dincer I, Cengel YA. Energy, **Entropy and Exergy Concepts and their Roles in Thermal Engineering.** *Entropy* 2001; **3**(3): 116-149. doi: 10.3390/e3030116

[14] Cai, L., Fu, Y., Cheng, Z., Xiang, Y., & Guan, Y. **Advanced Exergy and Exergoeconomic Analyses to Evaluate the Economy of LNG Oxy-fuel Combined Cycle Power Plant**. *Journal of Environmental Chemical Engineering* 2022; **10**(5): 108387. doi: 10.1016/j.jece.2022.108387

[15] Yağlı H., Koç Y., Kalay H., **Optimisation and Exergy Analysis of an Organic Rankine Cycle (ORC) Used as a Bottoming Cycle in a Cogeneration System Producing Steam and Power**. *Sustainable Energy Technologies and Assessments* 2021; **44**(10): 100985. doi: 10.1016/j.seta.2020.100985

[16] Soltani, S., Yari, M., Mahmoudi, S. M. S., Morosuk, T., & Rosen, M. A. **Advanced Exergy Analysis Applied to an Externally-Fired Combined-Cycle Power Plant Integrated with a Biomass Gasification Unit**. *Energy* 2013; **59**: 775-780. doi: 10.1016/j.energy.2013.07.038

[17] Medellín AA, Papayanopoulos EM, Millares CR. **Diagnosis and Redesign of Power Plants Using Combined Pinch and Exergy Analysis.** *Energy*, 2014; **72**(1): 643-651. doi: 10.1016/j.energy.2014.05.090

[18] Cihan A, Hacıhafızog˘lu O, Kahveci K. **Energy–Exergy Analysis and Modernization Suggestions for a Combined-Cycle Power Plant**. *International Journal of Energy Research* 2006; **30**(2): 115-126, doi: 10.1002/er.1133

[19] Reddy BV, Mohamed K. **Exergy Analysis of a Natural Gas Fired Combined Cycle Power Generation Unit**. *International Journal of Exergy* 2007; **4**(2): 180 – 196. doi: 10.1504/IJEX.2007.012065

[20] Ameri M, Ahmadi P, Khanmohammadi S. **Exergy Analysis of a 420 MW Combined Cycle Power Plant**. *International Journal of Energy Research*, 2008; 32(2): 175–183. doi: 10.1002/er.1351

[21] Açıkkalp E, Arasb H, Hepbasli A. **Advanced Exergy Analysis of an Electricity-Generating Facility Using Natural Gas.** *Energy Conversion and Management* 2014; **82**: 146-153. doi: 10.1016/j.enconman.2014.03.006

[22] Dincer I, Rosen MA. ***Exergy: Energy, Environment and Sustainable Development***, 2nd ed., *Newnes*, 2012.

[23] Bejan A, Tsatsaronis G, Moran M. ***Thermal design and optimization***. *John Wiley & Sons*, 1995.

[24] Pal R**. Chemical Exergy of Ideal and Non-Ideal Gas Mixtures and Liquid Solutions with Applications**. *International Journal of Mechanical Engineering Education* 2019; **47**(1): 44-72. doi: 10.1177/0306419017749581.

[25] Jimenez-Navarro, J. P., Kavvadias, K., Filippidou, F., Pavičević, M., & Quoilin, S. **Coupling the Heating and Power Sectors: The Role of Centralised Combined Heat and Power Plants and District Heat in a European Decarbonised Power System**. *Applied Energy*, 2020; **270**: 115134. doi: 10.1016/j.apenergy.2020.115134.

[26] Mollenhauer E, Christidis A, Tsatsaronis G. **Evaluation of an Energy-and Exergy-Based Generic Modeling Approach of Combined Heat and Power Plants**. *International Journal of Energy and Environmental Engineering* 2016; **7**(2): 167-176. doi: 10.1007/s40095-016-0204-6

[27] Doury RRJA, Mengüç MP. **Static and Dynamic Analyses for the Exergetic, Exergoeconomic and Environmental Assessment of a High-Performance Building**. *International Journal of Exergy* 2018; **27**(3): 393-418. doi: 10.1504/IJEX.2018.095409.